Evaluation of Stimulation Waveforms for Safe and Efficient Peripheral Nervous System Activation

Louis Regnacq, Roland Giraud, Arianna Ortega Sanabria, Anil Thota, Laure Roversi, Morteza Rouhani, Laura Mcpherson, James J Abbas, Ranu Jung, Olivier Romain, et al.

Evaluation of Stimulation Waveforms for Safe and Efficient Peripheral Nervous System Activation

Louis Regnacq, Roland Giraud, Arianna Ortega Sanabria, Anil Thota, Laure Roversi, Morteza Rouhani, Laura McPherson, James J. Abbas, Ranu Jung, Olivier Romain, Sylvie Renaud, Yannick Bornat, and Florian Kolbl

***Abstract*—Recent clinical trials have demonstrated the feasibility of using implantable neural stimulators for advanced therapies. However, to reduce long term deterioration of biological tissue, the amount of injected charge needs to be limited. Also, the stimulation has to be energy and power efficient to reduce battery dimensions and to maximize its lifetime. Several studies demonstrate that rectangular stimuli are not optimal regarding those criterion, and alternative waveforms have been proposed. In this report, a comparison between conventional rectangular stimuli and sinusoidal excitation is presented. We used *in-silico* models and *in-vivo* rodent experiments to determine excitation thresholds and injected charge per phase for both waveforms. Both studies demonstrated that, despite having higher thresholds, sinusoidal stimulation required less injected charge per phase, thus suggesting that it is a safer paradigm. Finally, energy and power consumption measurements were obtained and analysed. Peak power analysis does not provide any indication in favour of rectangular stimuli or sinusoidal stimulation. On the other hand, the stimulus energy plot demonstrates that sinusoidal excitation is globally more energy efficient than the traditional rectangular pulse and identifies an optimal stimulation zone.**

***Index Terms*—Neural stimulators, energy efficiency, implantable simulator, biphasic pulse, sinusoidal stimulation.**

I. Introduction

The network of peripheral nerves presents remarkable potential for modulating and/or monitoring the functioning of internal organs or the brain. The number of diseases and disabilities treated with implantable medical devices has massively increased in the past decade. Implantable neural stimulators treat thousands of patients with various neurological disorders such as chronic pain [1] or epilepsy [2]. Recent clinical investigations demonstrated huge potential of neuro-stimulation for advanced treatments such as restoring somatosensation for people with amputation [3] or visual sensation for people who are blind [4].

Neural stimulators artificially elicit neural activity by injecting a current stimulus to a selected area, aiming to locally depolarize targeted fibers' membrane. The parameters of injected current stimulus are specified and programmed by physicians to obtain the desired outcome and to minimize side effects

L. Regnacq, R. Giraud, L. Roversi, O. Romain and F. Kolbl are with the laboratory ETIS, UMR 8051, CY Cergy Paris Université, ENSEA, Cergy, France (contacts: louis.regnacq@ensea.fr, florian.kolbl@ensea.fr).

A. Ortega Sanabria, A. Thota, and Ranu Jung are with Adaptive Neural Systems Laboratory, Florida International University, Miami, United States.

M. Rouhani and J. J. Abbas are with the Center for Adaptive Neural Systems, Arizona State University, Tempe, United States

L. McPherson is with Washington University, St. Louis, United States

S. Renaud and Y. Bornat are with Univ. Bordeaux, Bordeaux INP, IMS CNRS UMR 5218, Aquitaine, Talence, France

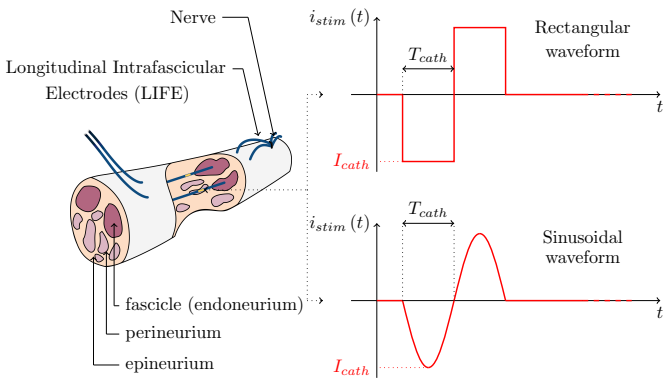

Fig. 1. Proposed *in-silico* and *in-vivo* studies, for comparison of both biphasic cathodic first rectangular and sinusoidal stimulation waveshapes.

[5]. Conventionally used biphasic pulses can be decomposed in two steps (Fig. 1). First a cathodic current pulse with defined amplitude and duration is delivered to induce firing of targeted fibers. Then, active charge balancing is obtained with an anodic pulse, reducing the risk of tissue damage due to electrochemical reactions.

However, others parameters have to be taken into account. On one hand, reducing the amount of injected charge decreases the risk of tissue deterioration , thus the stimulus needs to be charge efficient. On the other hand, power efficiency as well as energy efficiency are critical for battery-powered implanted neural stimulator to reduce constraints on the volume and lifetime of the battery.

Several studies on charge efficiency, power efficiency and energy efficiency have been carried out in the past. A global overview of the presented results suggests that rectangular biphasic stimulus is not optimal relative to theses three parameters. Alternative waveforms aiming to outperform rectangular waveform have been introduced, such as the rising exponential stimulus [6] or rising ramp waveform [7]. In [8] and [9], authors demonstrated that using sinusoidal-shaped stimuli instead of biphasic rectangular pulses for stimulation results is a safer and more energy efficient means of stimulation. However, those studies are based on *in-silico* modeling, and to the best of our knowledge, there are no similar *in-vivo* studies considering excitation with short pulse width sinusoidal stimulus instead of rectangular pulses.

In this report, we explore the possibility of exciting myelinated axons using sinusoidal stimulation and longitudinal intrafascicular electrodes (LIFEs), and compare it with the

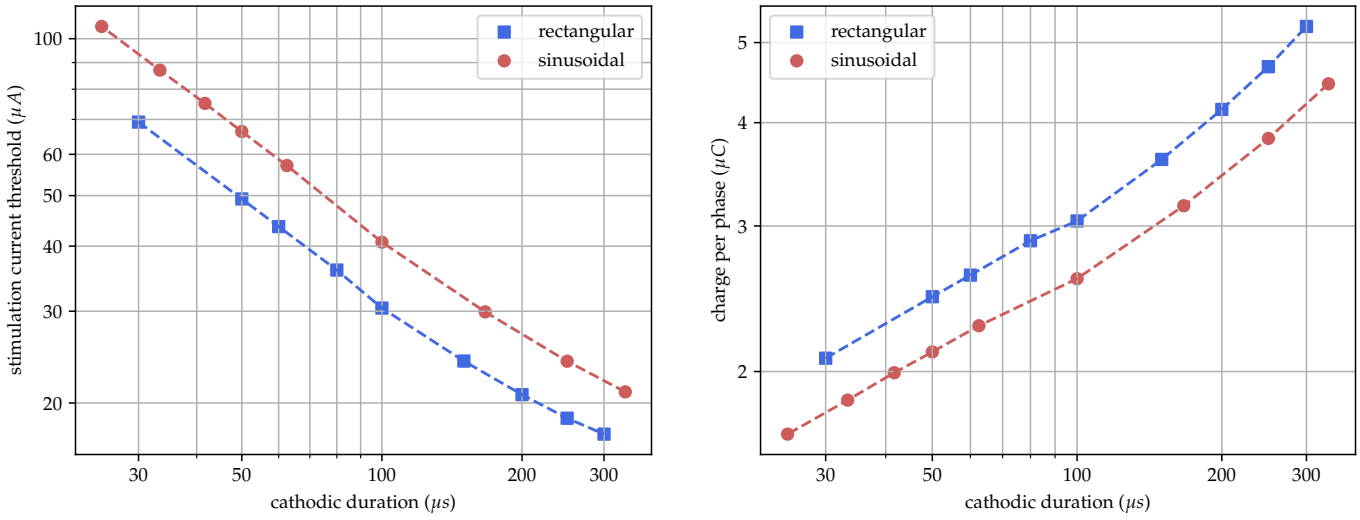

(a) (b)

Fig. 2. (a) Stimulation thresholds (I_{cath} notation as illustrated in Fig. 1), in μA, for the rectangular and sinusoidal as a function of the cathodic duration, T_{cath} in μs - for an axon diameter of $10\mu m$ and an electrode distance of 250 μm (b) Charge per phase in μC as a function of the stimulation cathodic duration for an axon diameter of $10\mu m$ and an electrode distance of 250 μm.

conventionally used biphasic rectangular pulse (Fig. 1). Excitation threshold and corresponding injected charges per phase were determined and analysed for both sinusoidal and biphasic stimuli with an *in-silico* model. A corresponding study was performed *in-vivo* on a rodent model to validate our model's predictions. Charge efficiency, power efficiency and energy efficiency were assessed and compared experimentally for the two studied stimulus waveforms when delivered by a stimulator on electrodes.

The report is organized as follows. Section II presents the model-based method and the obtained results, and Section III presents the *in-vivo* method and validation. Stimulation efficiency comparison is presented in Section IV and conclusions are drawn in Section V.

II. Model-based comparison of squared and sinusoidal stimulation waveshapes

A. Waveform parameters

Both compared stimulus are depicted in Fig. 1. All waveforms are biphasic and charge-balanced, without DC-offset current. All waveforms are cathodic (*i.e.* negative current) first. The rectangular waveform consists in two symmetrical constant current steps, with a cathodic duration of T_{cath}, without an interphase gap. The sinusoidal shape simply consists in one period of a negative sinusoid, with a period of $2 \cdot T_{cath}$. The cathodic current I_{cath} denotes the peak amplitude in the case of the sinusoidal shape, as illustrated in Fig. 1.

B. Method

The modeling approach follows the proposed methodology in [10]. The extracellular potential to the axon has been computed with Finite Element Method using COMSOL Multiphysics® 5.5. All computations have been performed under the quasi static approximation, which have been previously demonstrated to be valid even for frequencies in

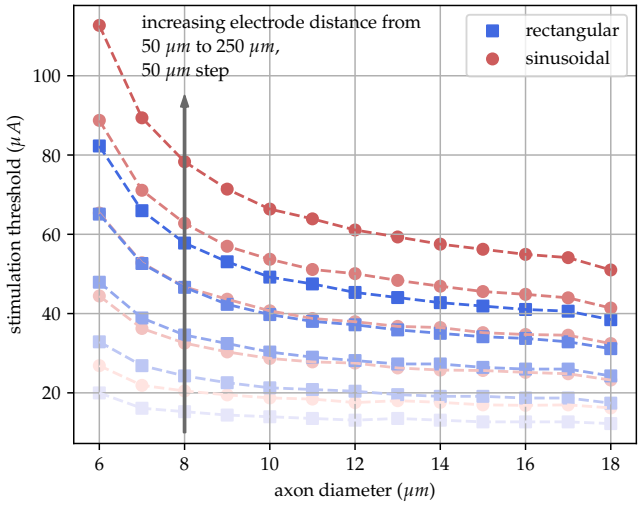

Fig. 3. Stimulation thresholds in μA as a function of the axon diameter and electrode distance, for both sinusoidal and rectangular waveforms.

the range of tens of kHz [11]. The nerve has been described as cylindrical (diameter of $800\mu m$) with a single axon fascicle (diameter of $600\mu m$) isolated by a perineurium sheet of $5\mu m$. The nerve was considered in a large saline solution box (diameter $10mm$). Material electrical properties were considered linear and are taken from [12]. The perineurium has been modeled as a thin layer [13]. All boundary conditions have been specified as in [14]. The LIFE electrode geometry consists in a cylinder of diameter of $25\mu m$ with an active site of $1mm$ in length [15]. The external sides of the saline solution box have been grounded.

Axon dynamics were computed using the MRG model [16] implemented on the NEURON software [17]. All axon lengths have been specified to perform a simulation on 20 nodes of Ranvier. The electrode center was placed in front of the tenth

node of Ranvier. The computational time step was set to $1\mu s$. A particularly high density spatial discretisation was chosen to take into account the possibility of high frequency phenomena, we chose to set the d-lambda rule frequency as defined in [17] (linked with the maximal frequency of sodium channels responsible for the depolarization) to 4 times the stimulation pattern frequency. All stimulation thresholds were investigated using a binary search on stimulation amplitude value, with a tolerance of $0.1\mu A$.

C. Results

The current thresholds for both the rectangular and sinusoidal waveforms has been computed as a function of the stimulation cathodic time T_{cath}, and is plotted in Fig. 2(a). For the entire covered pulse width range, the sinusoidal current threshold is higher than the rectangular one. The sinusoidal to rectangular threshold ratio r_I remains stable:

$$r_I = \frac{I_{cath\ sinusoidal}}{I_{cath\ rectangular}} \approx 1.33 \tag{1}$$

As expected, shorter stimulation waveforms require larger current amplitudes to trigger the axon.

For each waveform, we computed the charge per phase defined by:

$$Q_{per\ phase} = \int_0^{T_{cath}} i_{stim}\,(t)\ dt \tag{2}$$

In our two cases, this quantity can be expressed as:

$$Q_{per\ phase} = \begin{cases} I_{cath} \cdot T_{cath} & \text{if rectangular} \\ \dfrac{2 \cdot I_{cath} \cdot T_{cath}}{\pi} & \text{if sinudoidal} \end{cases} \tag{3}$$

Combining equations 1 and 3 leads to a sinusoidal to rectangular charge per phase ratio of:

$$\frac{Q_{per\ phase\ sinudoidal}}{Q_{per\ phase\ rectangular}} = \frac{2r_I}{\pi} \approx 0.85 < 1 \tag{4}$$

on average. This result is also validated by the computational results as depicted in Fig. 2(b), where the relative locations of the curves are inverted compared to Fig. 2(a). As a consequence, triggering an axon with a sinusoidal waveform consumes less charge per stimulation, which suggests safer stimulation [18], [19], especially for long term tissue safety. Moreover, decreasing the stimulation cathodic duration also decreases the charge required to trigger the axon.

In order to compare the behaviour of the sinusoidal and rectangular stimulations, we performed sweeps on the axons diameters (from 6 to $18\mu m$ corresponding to the mid range for mammals [20]), for electrode distances ranging from 50μ to $250\mu m$. Results are shown in Fig. 3. As already explained, the sinusoidal thresholds are higher, and the ratio r_I remains stable for both diameter and electrode distance variations.

Thus, changing the stimulation from rectangular biphasic to sinusoidal waveform lead to lower charge per phase and increased tissue safety without radically changing the stimulation paradigm.

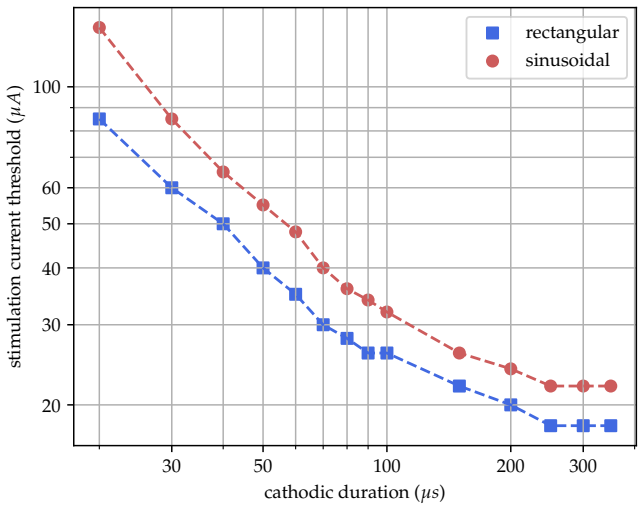

Fig. 4. *In-vivo* measured threshold, in μA, for both the biphasic and sinusoidal stimulation as a function of the stimulation the cathodic duration in μs.

III. In-vivo validation

A. Method

In-vivo acute experiments on rodent model were carried out with the same LIFE electrode implemented in our computational model [15]. Electrodes were implanted in the sciatic nerve of an anesthetized adult rat (Sprague Dawley, male, wheight 283 g, $0.5-3\%$ isoflurane in O_2) accessed through a lateral incision of the left hindlimb thigh. The muscles were retracted, the nerve isolated from the surrounding connective tissue, and an epineural dissection used to expose the fascicles and visualize the bands of Fontana. Vessel loops were used to lift the nerve under slight tension and using tungsten needles. LIFEs were threaded into the tibial fascicle parallel to the axons. The needles were cut and discarded after the LIFEs were inserted and the electrodes secured to the epineurium with 9-0 non-absorbable sutures. The muscle layers and skin were closed using 5-0 non-absorbable sutures and surgical staples, respectively.

Both rectangular and sinusoidal waveforms tested *in-silico* were then implemented on a custom current stimulator dedicated for arbitrary waveform stimulation. This stimulation platform is fully described in [21]. Strength-Duration curves were obtained for both waveform shapes. The pulse width of the rectangular stimulus, T_{cath}, was increased from $20\mu s$ to $100\mu s$ in steps of $10\mu s$, then in steps of $50\mu s$ until $350\mu s$. Stimulus repetition frequency was set to $1Hz$. For each pulse width, the stimulation current was increased until a visible muscle twitch was elicited. The same procedure was repeated with a sinusoidal stimulus.

B. Results

The measured current thresholds of both the rectangular biphasic and sinusoidal stimulus waveforms are depicted in Fig. 4. Both stimuli follow the same tendency: decreasing pulse width increases stimulation threshold. This tendency was also shown by our computational study. *In-vivo* measured

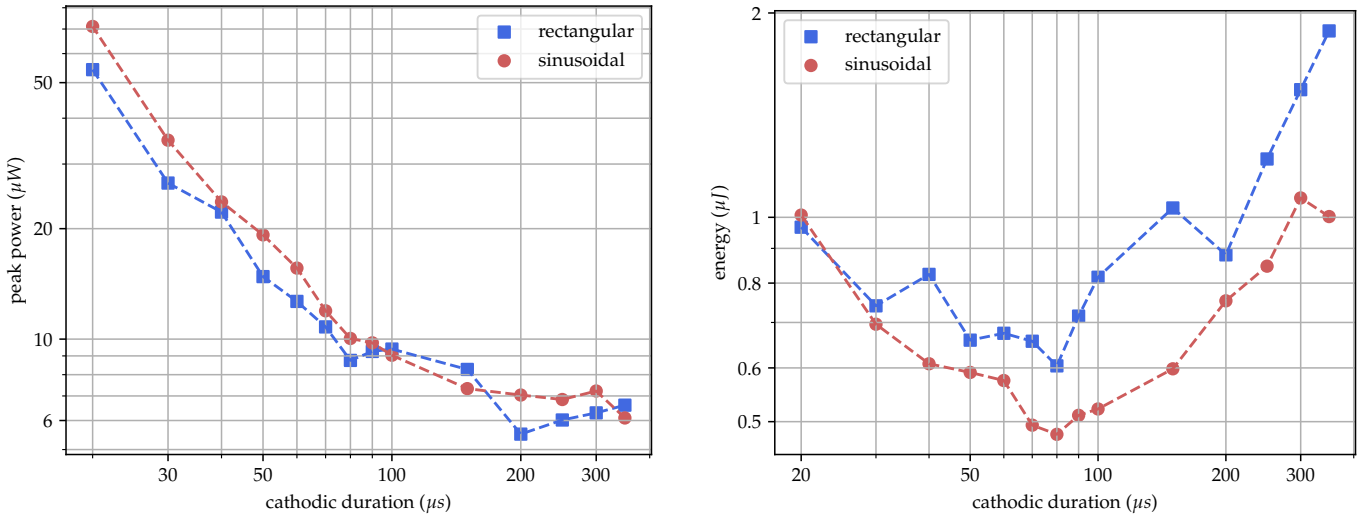

(a) (b)

Fig. 5. (a) Peak power of the stimulus waveforms for the current threshold obtained with the *in-vivo* experiment, with the exact waveforms applied on LIFE electrode in saline solution(b) Energy of the stimulus for the current threshold obtained with the *in-vivo* experiment.

thresholds are very close to the thresholds obtained *in-silico*: from $135\mu A$ to $22\mu A$ for the sinusoidal stimulus, and $85\mu A$ to $18\mu A$ for the rectangular biphasic pulse (resp. $105\mu A$ to $21\mu A$ and $69\mu A$ to $17\mu A$ for the *in-silico* study). Finally, the mean ratio between rectangular stimulation and sinusoidal stimulation is equal to 1.30 with a standard deviation of 0.11. This ratio is similar to the one computed by the *in-silico* model, the charge ratio is then approximately 0.82. This leads to a practical 18% charge saving stimulation with the sinusoidal waveform.

IV. Impact on Peak-Power and Energy Consumption

A. Method

To compare power and energy consumption of the two stimuli, the same LIFE electrode was placed in saline solution with a conductivity of approximately $1.6S/m$. Electrode voltage has been recorded via an instrumentation amplifier (AD8250, Analog Devices). Current through the electrode has been recorded via a transimpedance amplifier build around a dedicated op-amp (THS4631, Texas Instrument). Both current and voltage were then synchronously converted to the digital domain with a 14-bit, $100MSps$ dual channels ADC (AD9648, Analog Devices, embedded on the Analog Discovery 2 platform from Digilent). Instantaneous power and energy were determined for each value of current threshold reported in Fig. 4.

B. Results

Fig 5(a) illustrates the peak power of both stimulus as a function of cathodic duration. For both excitation methods, peak power decreases with stimulation cathodic duration. The peak power of rectangular stimulation goes from $54\mu W$ for a $20\mu s$ cathodic duration stimuli, to $6.6\mu W$ for a $350\mu s$ stimuli. The peak power of sinusoidal stimulation goes from $71\mu W$ for a $20\mu s$ cathodic duration, to $6.0\mu W$ for a $350\mu s$ stimuli. Peak power is mainly affected by the current amplitude of the stimulation and the electrode impedance. Electrode impedance decreases with frequency [22], thus for a constant stimulation current, a decrease in peak power is expected. However, the augmentation of stimulation threshold with frequency counteracts the decline in impedance, resulting in an overall increase in peak power. Fig 5(a) does not particularly distinguish rectangular excitation from sinusoidal excitation. One can note that the current-voltage relationship of an electrode tends to be non-linear [22], thus an analytical accurate prediction of power and energy is not trivial.

Fig 5(b) presents the energy required for both stimulus in regard of the cathodic duration. The two waveforms exhibit similar behavior. First, a decrease in energy is noticed: from $0.96\mu J$ for the rectangular pulse and $1.0\mu J$ sinusoidal pulse, for a $20\mu s$ cathodic duration stimuli to a minimum of $0.6\mu J$ for the rectangular pulse and $0.47\mu J$ for the sinusoidal excitation, when the cathodic duration is about $80\mu s$.

Then, an increase in energy is observed, reaching $1.9\mu J$ and $1.0\mu J$ for the rectangular stimuli and sinusoidal stimuli respectively, with a cathodic duration of $350\mu s$. Globally, the energy required for sinusoidal stimulation is lower than the energy required with rectangular stimuli. This result suggests that choosing a stimulation pulse width of about $80\mu s$ optimizes stimulation in term of energy efficiency. This result also suggests that, for the same optimal stimulation parameters, choosing sinusoidal excitation would lead to more energy efficient stimulation than with rectangular excitation.

V. Conclusion and Perspectives

In this contribution, we performed an extensive comparison of two waveforms: rectangular and sinusoidal current stimuli. Our approach utilized *in-silico* and *in-vivo* evaluations for both physiological and electrical performances of both shapes. Unlike previous reported comparisons [6], [7], this study is

not based on electrode impedance models but actual recording of the electrical behaviour of stimuli on electrodes loads. We developed this protocol in order to take into account non-linear and complex phenomena from physiological and electrical responses to the stimuli.

This comprehensive comparison between these two waveforms highlight some counter-intuitive results. If the stimulation with sinusoidal current requires higher activation current threshold, the overall stimulation process is safer for long term experiments. Moreover, this increased tissue safety comes with a lower energetic cost and without affecting significantly the peak power that stimulation circuits have to deliver. Depending on the exact load, here a LIFE electrode, an energetic optimum can be identified in term of stimulation parameters.

Intrafascicular electrodes require much smaller current amplitude to elicit neural activity than commonly used extrafascicular such as CUFF electrodes [23]. Tens of μA are sufficient to generate a visible muscle twitch on a rodent model. Longer pulse widths would require even less current but the neural stimulator used in this study does not provide sufficient resolution to generate such low current waveforms accurately. Designing a neural stimulator targeting neural stimulation on LIFE electrodes would need to address this point. A low current stimulation combined with a low electrode impedance at the considered pulse width results in about $1.1V$ peak to peak voltage for the worst case scenario. Thus, a large voltage compliance is no longer required for the stimulating device. Designing an application specified integrated circuit (ASIC) for LIFE electrodes is possible with a standard CMOS process, without using high-voltage processes, lowering the cost while offering better performances.

The generation of sinusoidal waveform requires additional hardware resources. This additional complexity increases the global power consumption, and could limits the overall energy efficiency of sinusoidal stimulation. Nevertheless, advanced CMOS processes with compatible voltage compliance allow the design of very low-consumption sinewave generator based on highly efficient strategy such as $\Delta\Sigma$ modulation [24], thus limiting the supplementary consumption cost of neurostimulation with sine-shaped pulses.

With our method to investigate the impact of waveform shape, we intend to design safer protocols for complex stimulation scenarios. The next steps in our work will be a larger comparison of different waveforms with different frequency content for axonal excitation [6]. Validation on a larger rodent group is also required to obtain statistically representative data. Ultimately, we will consider this overall method in other stimulation paradigms such as blocking mechanisms [25].

ACKNOWLEDGEMENT

This research is part of the BioTIFS (*Improved Selectivity for **Bio**electronic **T**herapies with **I**ntrafascicular **S**timulation*) project, and is supported by the Collaborative Research in Computational Neuroscience (CRCNS), by the the American National Institutes of Health (NIH-R01-EB027584) and the French *Agence Nationale pour la Recherche* (ANR-18-NEUC-0002-02).

REFERENCES

[1] X. Moisset, M. Lanteri-Minet, and D. Fontaine, "Neurostimulation methods in the treatment of chronic pain," *Journal of Neural Transmission*, vol. 127, no. 4, pp. 673–686, Apr. 2020.

[2] R. S. Fisher and A. L. Velasco, "Electrical brain stimulation for epilepsy," *Nature Reviews Neurology*, vol. 10, no. 5, pp. 261–270, May 2014.

[3] S. J. Bensmaia, D. J. Tyler, and S. Micera, "Restoration of sensory information via bionic hands," *Nature Biomedical Engineering*, 2020.

[4] A. Barriga-Rivera, T. Guo, C.-Y. Yang, A. A. Abed, S. Dokos, N. H. Lovell, J. W. Morley, and G. J. Suaning, "High-amplitude electrical stimulation can reduce elicited neuronal activity in visual prosthesis," *Scientific Reports*, vol. 7, no. 1, p. 42682, Feb. 2017.

[5] D. R. Merrill, M. Bikson, and J. G. Jefferys, "Electrical stimulation of excitable tissue: design of efficacious and safe protocols," *Journal of neuroscience methods*, vol. 141, no. 2, pp. 171–198, 2005.

[6] S. Ethier and M. Sawan, "Exponential current pulse generation for efficient very high-impedance multisite stimulation," *IEEE Transactions on Biomedical Circuits and Systems*, vol. 5, no. 1, pp. 30–38, 2011.

[7] A. Wongsarnpigoon, J. P. Woock, and W. M. Grill, "Efficiency analysis of waveform shape for electrical excitation of nerve fibers," *IEEE Transactions on Neural Systems and Rehabilitation Engineering*, vol. 18, no. 3, pp. 319–328, 2010.

[8] M. Sahin and Y. Tie, "Non-rectangular waveforms for neural stimulation with practical electrodes," *Journal of neural engineering*, vol. 4, no. 3, pp. 227–233, Sep. 2007, edition: 2007/05/02.

[9] T. J. Foutz and C. C. McIntyre, "Evaluation of novel stimulus waveforms for deep brain stimulation," *Journal of Neural Engineering*, vol. 7, no. 6, p. 066008, Nov. 2010, publisher: IOP Publishing.

[10] S. Romeni, G. Valle, A. Mazzoni, and S. Micera, "Tutorial: a computational framework for the design and optimization of peripheral neural interfaces," *Nature Protocols*, vol. 15, pp. 3129–3153, Oct. 2020.

[11] C. A. Bossetti, M. J. Birdno, and W. M. Grill, "Analysis of the quasi-static approximation for calculating potentials generated by neural stimulation," *Journal of neural engineering*, vol. 5, no. 1, p. 44, 2007.

[12] J. B. Ranck and S. L. BeMent, "The specific impedance of the dorsal columns of cat: an anisotropic medium," *Experimental neurology*, vol. 11, no. 4, pp. 451–463, 1965.

[13] N. A. Pelot, C. E. Behrend, and W. M. Grill, "On the parameters used in finite element modeling of compound peripheral nerves," *Journal of Neural Engineering*, vol. 16, p. 016007, Feb. 2019.

[14] N. A. Pelot, B. J. Thio, and W. M. Grill, "Modeling current sources for neural stimulation in comsol," *Frontiers in computational neuroscience*, vol. 12, p. 40, 2018.

[15] A. K. Thota, S. Kuntaegowdanahalli, A. K. Starosciak, J. J. Abbas, J. Orbay, K. W. Horch, and R. Jung, "A system and method to interface with multiple groups of axons in several fascicles of peripheral nerves," *Journal of neuroscience methods*, vol. 244, pp. 78–84, 2015.

[16] C. C. McIntyre, A. G. Richardson, and W. M. Grill, "Modeling the excitability of mammalian nerve fibers: influence of afterpotentials on the recovery cycle," *Journal of neurophysiology*, vol. 87, no. 2, pp. 995–1006, 2002.

[17] N. T. Carnevale and M. L. Hines, *The NEURON book*. Cambridge University Press, 2006.

[18] R. V. Shannon, "A model of safe levels for electrical stimulation," *IEEE Transactions on biomedical engineering*, vol. 39, no. 4, pp. 424–426, 1992.

[19] R. Jung, J. J. Abbas, S. Kuntaegowdanahalli, and A. K. Thota, "Bionic intrafascicular interfaces for recording and stimulating peripheral nerve fibers," *Bioelectronics in medicine*, vol. 1, no. 1, pp. 55–69, 2018.

[20] J. Badia, A. Pascual-Font, M. Vivó, E. Udina, and X. Navarro, "Topographical distribution of motor fascicles in the sciatic-tibial nerve of the rat," *Muscle and Nerve*, vol. 42, no. 2, pp. 192–201, 2010.

[21] F. Kolbl, Y. Bornat, J. Castelli, L. Regnacq, G. N'Kaoua, S. Renaud, and N. Lewis, "Ic-based neuro-stimulation environment for arbitrary waveform generation," *Electronics*, vol. 10, no. 15, 2021.

[22] F. Kölbl, J. Sabatier, G. N'Kaoua, F. Naudet, E. Faggiani, A. Benazzouz, S. Renaud, and N. Lewis, "Characterization of a non linear fractional model of electrode-tissue impedance for neuronal stimulation," in *2013 IEEE Biomedical Circuits and Systems Conference (BioCAS)*. IEEE, 2013, pp. 338–341.

[23] A. A. Leis, M. P. Schenk, A. A. Leis, and M. P. Schenk, "Model-based analysis and design of nerve cuff electrodes for restoring bladder function by selective stimulation of the pudendal nerve," *Atlas of Nerve Conduction Studies and Electromyography*, vol. 10, pp. 238–243, 2014.

[24] K. Kim, S. Kim, and H.-J. Yoo, "Design of sub-10-uw sub-0.1% thd sinusoidal current generator ic for bio-impedance sensing," *IEEE Journal of Solid-State Circuits*, pp. 1–1, 2021.

[25] Y. A. Patel and R. J. Butera, "Challenges associated with nerve conduction block using kilohertz electrical stimulation," *Journal of Neural Engineering*, vol. 15, no. 3, p. 031002, mar 2018.